Theoretical high-pressure equations of state and phase diagrams of the alkali metals

David A. Young and Marvin Ross
Lawrence Livermore National Laboratory, University of California, Livermore, California 94550
(Received 28 February 1983)

A two-parameter Heine-Abarenkov local pseudopotential is used to fit experimental room-temperature isotherms of lithium, sodium, and potassium up to pressures of 100 kbar. Lattice dynamics and one-component-plasma fluid variational theory are then used to compute solid-solid and solid-liquid phase boundaries, which are found to be in good agreement with experiment. The theoretical shock-compression Hugoniot curves differ significantly from experiment near 1 Mbar, and anomalously low values of the theoretical lattice Grüneisen parameter are obtained at very high compression. Further improvements in the theoretical models are suggested.

I. INTRODUCTION

In metals the long-range Coulomb interaction and the partially filled conduction bands lead to interatomic forces that are inherently many-body and unlike those for rare gases and small molecules in which two-body interactions dominate. As a result, practical calculations of the thermodynamic properties of metals remain a difficult problem. However, for certain metals pseudopotential theory provides a formalism which leads to an effective two-body interatomic potential, and which has proved of great value for calculating thermodynamic and transport properties.[1-3]

Pseudopotential models are most appropriate for nearly-free-electron metals such as Li, Na, K, Al, and Pb, in which the electrons in the conduction band are mainly of s and p character. Many model calculations have focused on the properties of alkali metals at 1 bar pressure. Although several workers have calculated the solid isothermal equations of state and shock-compression curves of the alkalis at high pressure,[4-7] there has not yet been a systematic application of the theory to all available experimental data.

Theoretical work is needed because there is now a substantial body of experimental high-pressure data on the alkalis, including isotherms,[8-12] melting curves,[13-15] and shock-compression Hugoniot curves.[16,17] With the rapid advances in static and dynamic high-pressure technologies, we can expect future experimental work reaching into the megabar pressure range.

In this paper we examine the usefulness of pseudopotential theory at high pressure by a systematic comparison of experimental Li, Na, and K data with theoretical predictions. Because the thermodynamic properties of rubidium and cesium depend on the more complex physics of d electrons, we do not consider these two metals here.

In local pseudopotential theory an electron-ion potential is determined from empirical considerations and then used in statistical-mechanical models to calculate thermodynamic properties. A proper evaluation of the method depends to a great extent on the accuracy of these models.

Our plan is first to determine the two parameters of a Heine-Abarenkov pseudopotential by fitting the 300-K experimental solid isotherm using the method of lattice dynamics. We then examine the accuracy with which the lattice-dynamics and fluid-variational theories predict the measured high-temperature and high-pressure thermodynamic properties. We find that in general there is good agreement between theory and experiment up to 100 kbar pressure, but that the theory becomes less accurate at still higher pressures.

In Sec. II we review the pseudopotential and the statistical-mechanical methods. These are used in Sec. III to calculate isotherms, phase diagrams, and Hugoniot curves for lithium, sodium and potassium. The overall results of the calculations are briefly discussed in Sec. IV.

II. PSEUDOPOTENTIAL AND STATISTICAL MODELS

The details of pseudopotential theory have been thoroughly discussed elsewhere[1-3] and we limit our remarks to some essential features. The model consists of N positively charged ions moving in a degenerate and nearly-free-electron gas of volume V. The electron-ion interaction is approximated by a local pseudopotential. Many pseudopotential forms have been suggested, but all have basically the same features. The electron-ion potential has a Coulomb form at long range, but this is modified in the short-range core region with a slowly-varying potential which replaces the Coulomb singularity. This core potential is introduced to represent the Pauli repulsion between the conduction electrons and the atomic core electrons. Different potential models differ in the treatment of the core region. In the pseudopotential theory, the potential perturbs the electron gas, leading to an accumulation of electrons around the ions and to a screened ion-ion pair potential.

We have chosen the two-parameter Heine-Abarenkov local pseudopotential for use in our calculations. Here the electron-ion interaction is given by

$$V(r)=\begin{cases}-\dfrac{Ze^2}{r}, & r\geq r_c \\ w_0, & r<r_c\end{cases} \tag{1}$$

 ©1984 The American Physical Society

with a Fourier transform

$$V(k)=\frac{4\pi}{k^2}\left[(-w_0 r_c - Ze^2)\cos(kr_c)+\frac{w_0}{k}\sin(kr_c)\right], \tag{2}$$

where Z is the number of valence electrons per atom. For the alkali metals we set $Z=1$. We regard this potential as a convenient semiempirical form which can be fitted to experimental thermodynamic data.

For this model an expression for the Helmholtz free energy has been derived that is correct to second order in the nearly-free-electron approximation. From this expression all of the thermodynamic functions may be obtained. The Helmholtz free energy per atom is

$$\frac{A}{N}=E_{\rm EG}+E_M+E_{\rm BS}+E_0+\frac{A_i}{N}, \tag{3}$$

where $E_{\rm EG}$ is the $T=0$ K energy of the electron gas, E_M is the Madelung energy of point ions in a uniform negative background, $E_{\rm BS}$ is the band-structure energy arising from the screened pseudopotential, E_0 is the Hartree energy, which appears as the result of omitting the $k=0$ term in $E_{\rm BS}$, and A_i is the contribution to the free energy arising from the ionic motion.

The electron-gas energy is given by

$$E_{\rm EG}=E_k+E_{\rm XC}, \tag{4}$$

where

$$E_k=\frac{3}{5}\left[\frac{9\pi}{4}\right]^{2/3}\frac{Z}{r_s^2}, \tag{5}$$

$$E_{\rm XC}=-1.03937\left[\frac{Z}{r_s^{0.913\,93}}\right] \tag{6}$$

(in Rydberg units), and

$$r_s=\left[\frac{3V}{4\pi NZ}\right]^{1/3}a_0^{-1}.$$

(in bohr). Here E_k is the kinetic energy of the free-electron gas, and $E_{\rm XC}$ is an accurate representation[18] of the exchange-correlation energy of the electron gas. The parameter r_s is the electron-sphere radius and $a_0=0.529\,177\times10^{-8}$ cm is the Bohr radius. These energies are volume dependent only and are independent of the phase of the metal. We can safely use the zero-Kelvin value of $E_{\rm EG}$ as long as the temperature is much less than the Fermi temperature, which in the alkali metals is of order 10^4-10^5 K.

In the solid, the Madelung energy E_M is known very accurately for the three solid phases considered here[19]:

$$\begin{aligned}
&\text{bcc: } E_M=-1.791\,858\,52\frac{Z_2}{r_A},\\
&\text{fcc: } E_M=-1.791\,747\,23\frac{Z^2}{r_A},\\
&\text{hcp: } E_M=-1.791\,676\,24\frac{Z^2}{r_A}
\end{aligned} \tag{7}$$

(in Ry), where r_A is the Wigner-Seitz or ion-sphere radius,

$$r_A=\left[\frac{3V}{4\pi N}\right]^{1/3}a_0^{-1}$$

(in bohr). Here the hcp value corresponds to the ideal c/a ratio, $c/a=(8/3)^{1/2}$.

In the solid, the band-structure term[3] is given by

$$E_{\rm BS}=\frac{N}{2V}\sum_{k=K}V(k)^2\frac{k^2}{8\pi}\left[\frac{1}{\epsilon(k)}-1\right] \tag{8}$$

(in Ry). Here the sum is taken over all reciprocal-lattice distances K, with $K=0$ omitted. The dielectric function $\epsilon(k)$ is given by the Lindhard approximation,[3]

$$\epsilon(k)=1-\left[\frac{8\pi}{k^2}\right]X(k), \tag{9}$$

where

$$\begin{aligned}
&X(k)=-\frac{k_F}{2\pi^2}\left[\frac{1}{2}+\frac{(1-y^2)}{4y}\ln\left|\frac{(1+y)}{(1-y)}\right|\right],\\
&y=\frac{k}{2k_F},
\end{aligned} \tag{10}$$

and

$$k_F=\left[\frac{9\pi}{4}\right]^{1/3}r_s^{-1}$$

(in bohr^{-1}). We have not introduced exchange and correlation into the dielectric function because we wish to examine the adequacy of the pseudopotential theory in its simplest form. In practice, the sum $E_{\rm BS}$ is accurately approximated by a sum over several thousand reciprocal-space neighbors in a spherical volume, plus an integral over the remaining infinite volume.

The Hartree energy for the Heine-Abarenkov potential is the positive electrostatic energy arising from the difference between the pseudopotential [Eq. (1)] and the pure Coulomb potential:

$$E_0=\frac{NZ\pi r_c^3}{V}\left[\frac{4w_0}{3}+\frac{4Z}{r_c}\right] \tag{11}$$

(in Ry). This term, like $E_{\rm EG}$, is independent of the phase of the metal.

The lattice-vibrational free energy A_i is computed by quasiharmonic lattice dynamics.[3] In our lattice-dynamics model, an irreducible wedge of the first Brillouin zone is sampled with $\vec{\rm k}$ vectors, dynamical matrix elements $D_{ij}(\vec{\rm k})$ are computed, and this matrix is diagonalized to obtain the frequencies $\nu_i(\vec{\rm k})$. Then

$$\frac{A_i}{N}=\sum_{i=1}^{3N}\left\{kT\ln\left[1-\exp\left[-\frac{h\nu_i}{kT}\right]\right]+\frac{h\nu_i}{2}\right\} \tag{12}$$

is approximated as a sum of weighted terms. The precision of A_i can be checked by varying the number of points in the Brillouin zone.

Other thermodynamic functions can be obtained readily

from the total free energy by standard thermodynamic relationships. Of specific interest here are the pressure $p=-(\partial A/\partial V)_T$ and the energy $E=[\partial(A/T)/\partial(1/T)]_V$.

For the liquid we use a variational theory which is based on the rigorous Gibbs-Bogolyubov inequality,

$$\frac{A_c}{N}\leq\frac{A_0}{N}+\langle H_c-H_0\rangle_0 . \tag{13}$$

This means that the true configurational free energy A_c is bounded above by the sum of the configurational free energy of a reference system, A_0, and the average of the difference between the actual and reference potential energies, taken over all reference configurations. If the reference system is close to the actual system, then the perturbation will be small and the theory will be accurate.

Such a reference system is the one-component plasma (OCP) fluid. The OCP variational theory has been developed and tested against Monte Carlo calculations by Ross *et al.*[20] For the OCP reference system the inequality is

$$\frac{A_c}{NkT}\leq\frac{A_0(\Gamma')}{NkT}+\frac{\Gamma}{\pi}\int_0^\infty f(q)S_0(q,\Gamma')\left[\frac{1}{\epsilon(q)}-1\right]dq + \left[\frac{(\Gamma-\Gamma')}{\Gamma'}\right]\frac{U_0(\Gamma')}{NkT}+\frac{E_0}{kT} , \tag{14}$$

where

$$f(q)=\left[V(q)\frac{q^2}{8\pi Z}\right]^2 ,$$
$$q=kr_A , \tag{15}$$
$$\Gamma=\frac{Z^2e^2}{r_AkT} ,$$

and

$$\Gamma'=\frac{Z'^2e^2}{r_AkT} .$$

The OCP reference internal energy and free energy have been very accurately obtained from Monte Carlo calculations[21]:

$$\frac{U_0(\Gamma')}{NkT}=a\Gamma'+b(\Gamma')^{1/4}+c(\Gamma')^{-1/4}+d , \tag{16}$$

$$\frac{A_0(\Gamma')}{NkT}=a\Gamma'+4[b(\Gamma')^{1/4}-c(\Gamma')^{-1/4}] +d\ln\Gamma'-[a+4(b-c)]-0.436 . \tag{17}$$

Here we use the parameters[21] $a=-0.897\,913$, $b=0.952\,80$, $c=0.189\,07$, and $d=-0.817\,73$.

The OCP fluid structure factor $S_0(q,\Gamma')$ has been computed by F. J. Rogers at this laboratory using the hypernetted-chain (HNC) integral equation with bridge graph correction.[22] The integral-equation solutions for $0.1\leq\Gamma'\leq180$ and $0\leq q\leq25$ have been made into a table which is interpolated in Γ' space and then numerically integrated in q space according to Eq. (14). In Ref. 20 Ross *et al.* used an $S_0(q,\Gamma')$ table taken from Monte Carlo calculations. However, we have found that the scatter in these data was sufficient to cause pressure discontinuities of about 1 kbar in the calculated pressure. The present $S_0(q,\Gamma')$ is in excellent agreement with Monte Carlo calculations and has the advantage of smoothness.

The right-hand side of Eq. (14) is evaluated and minimized with respect to the variational parameter Γ', and this minimum value is taken to be equal to A_c/NkT. The total free energy per atom is then given by the sum of the configurational, electron-gas, and ideal-gas terms,

$$\frac{A}{N}=\frac{A_c}{N}+E_{\rm EG}-kT\ln\left[\frac{Ve}{N\Lambda^3}\right] , \tag{18}$$

where

$$\Lambda=\frac{h}{(2\pi mkT)^{1/2}} .$$

The configurational pressure and energy may be computed directly by using the value of Γ' at the minimum.[20]

III. CALCULATIONS

A. Isotherms

The pseudopotential parameters r_c and w_0 for Li, Na, and K are determined by fitting them to the experimental 300-K isotherms. This is done by fixing w_0 and varying r_c until $p(V=V_0,\ T=300\ \text{K})=0$ as computed by lattice dynamics for the bcc lattice. The resulting isotherms for a series of w_0 values are then compared with experiments up to 100 kbar and the parameter set in best agreement is chosen. At the same time, the total energy at $V=V_0$ is the binding energy (cohesive energy plus first ionization potential) and this can also be compared with experiment. The pseudopotential parameters and binding energies are shown in Table I.

The lithium isotherm is shown in Fig. 1. It was not possible to find parameters yielding a highly accurate fit to the experimental lithium[8-11] p-V curve. All theoretical isotherms were more or less too stiff. Also, the theoretical

TABLE I. Pseudopotential parameters, theoretical (theor) and experimental (expt) binding energies, and normal volumes for lithium, sodium, and potassium.

Element	r_c (bohr)	w_0 (Ry)	E_b (theor) (Ry)	E_b (expt) (Ry)	V_0 (cm^3/mol)
Li	1.70	−0.71	−0.546	−0.518	13.02
Na	2.20	−0.45	−0.456	−0.461	23.73
K	2.90	−0.29	−0.375	−0.385	45.61

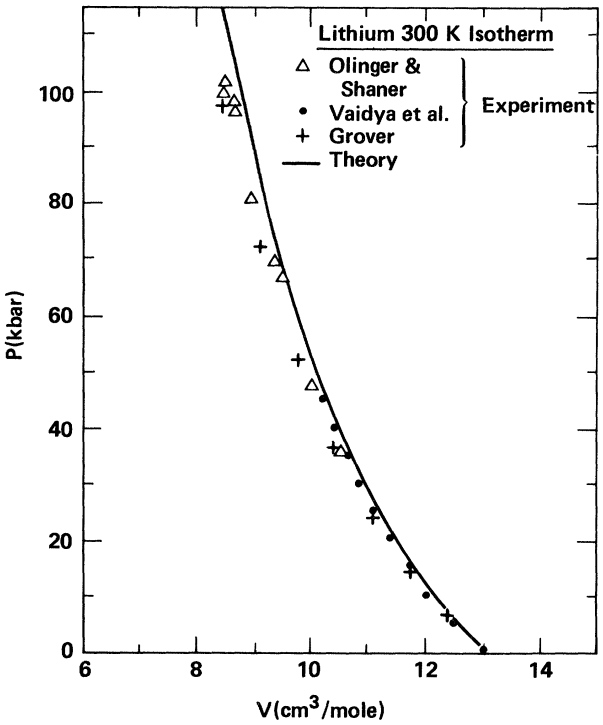

FIG. 1. Comparison of experimental and theoretical 300-K pressure-volume isotherms for lithium.

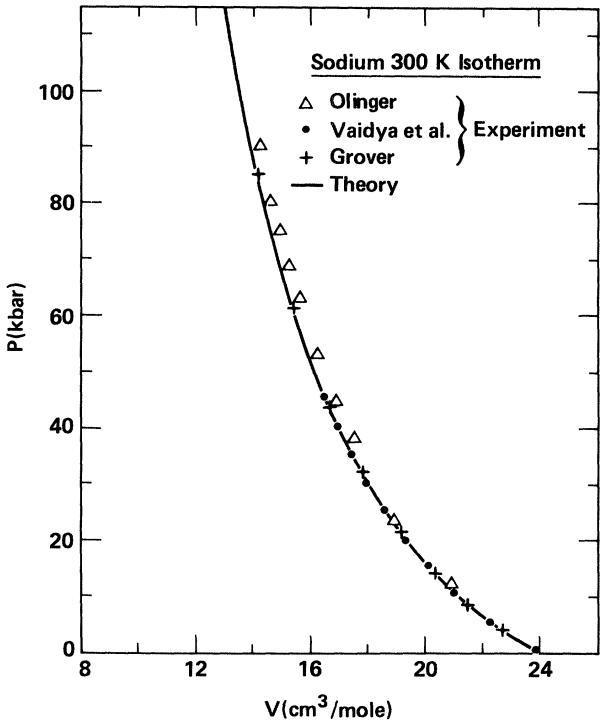

FIG. 2. Comparison of experimental and theoretical 300-K pressure-volume isotherms for sodium.

binding energy is substantially in error. These discrepancies may be ascribed to the inadequacy of the second-order theory for lithium.[23] In lithium the valence electrons have some $2p$ character but no p core state exists to keep them away from the nucleus. The second-order perturbation formalism does not adequately represent this strong pseudopotential, and the result is a theoretical ion-ion potential which is too repulsive and a theoretical isotherm which is too stiff. Third- and higher-order terms are needed for adequate treatment of lithium. The theoretical sodium and potassium isotherms can be fitted more accurately to experiment,[8–11] as shown in Figs. 2 and 3.

Having fitted the room-temperature solid isotherms with the pseudopotential, we can then test the liquid model by making predictions of higher-temperature liquid isotherms. This is done in Fig. 4, and the agreement between theory and experiment[12] for Na and K is good. We are unaware of comparable data for Li.

B. Phase diagrams

The pseudopotentials can now be used with the solid and liquid statistical-mechanical models to compute theoretical phase diagrams for the three metals. The standard method for obtaining a phase diagram is to plot the Gibbs free-energy isotherms of competing phases against pressure and to locate all crossing points. Each crossing point represents a P,T point on the phase diagram. However, this procedure is time consuming and instead we compute Helmholtz free-energy isotherms for each possible phase. The differences in Helmholtz free energy ΔA

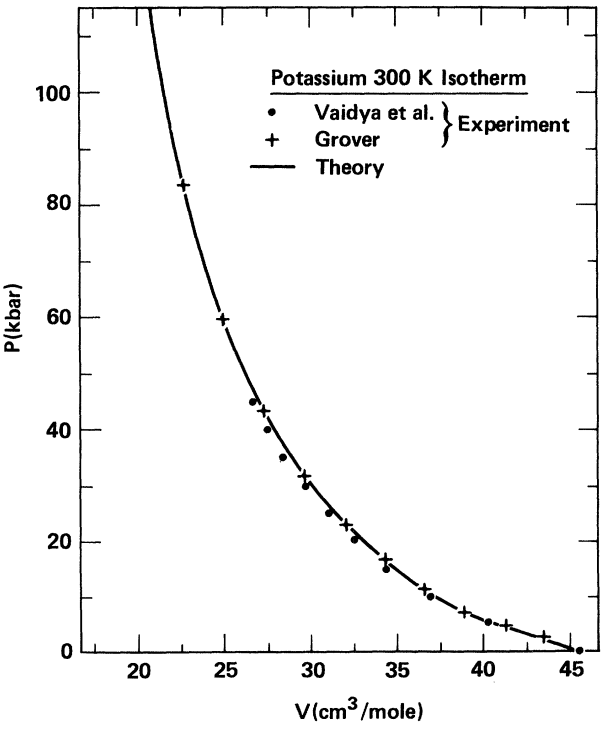

FIG. 3. Comparison of experimental and theoretical 300-K pressure-volume isotherms for potassium.

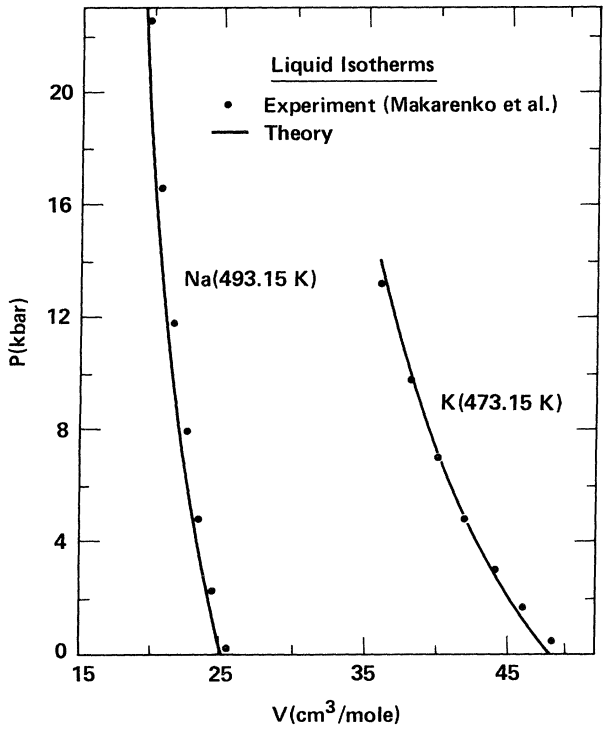

FIG. 4. Comparison of experimental and theoretical liquid isotherms for sodium and potassium.

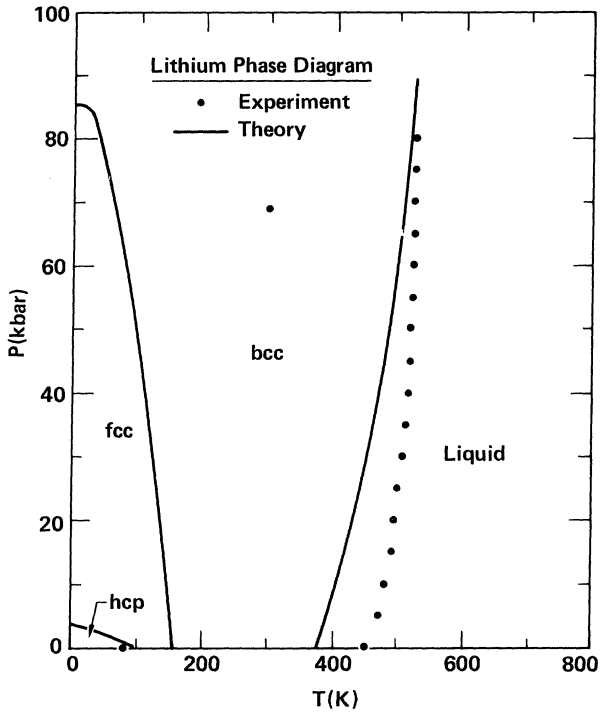

FIG. 5. Comparison of experimental and theoretical phase diagrams for lithium. Lithium shows a bcc to close-packed transition near 80 K and $p=0$, and a bcc to fcc transition at 300 K and 69 kbar.

between pairs of phases are then plotted as a function of volume and the crossing points $\Delta A=0$ will indicate the coexistence of two phases. The pressure of the transition can be estimated by averaging the pressures of the two coexisting phases at the volume where $\Delta A=0$. This is an excellent approximation in solid-solid transitions where the volume change across the transition is very small. It is less good for the melting curve, but the error is within 1 kbar even here.

For lithium, the results are shown in Fig. 5. The lattice-dynamics models predict fcc and hcp phases at low temperatures and a bcc phase at high temperatures. The experimental situation is somewhat ambiguous,[24] but fcc and hcp phases have been found in Li below 80 K. The experimental p-T solid-solid boundaries have not been determined at low temperatures. At room temperature and 69 kbar, a transition from bcc to fcc has recently been found.[9] It is presumed that a continuous fcc-bcc phase line starts at $p=0$ at low temperature, passes through $p=69$ kbar and $T=300$ K, and reaches a triple point on the melting curve.[9] This is not predicted by the theory because the bcc-fcc phase boundary is calculated to have a negative rather than a positive slope. The theoretical melting curve has too low a temperature at $p=0$ but approaches the experimental curve at high pressure.

The phase diagram for sodium is shown in Fig. 6. Lattice dynamics predicts a small region of fcc stability in the lower left corner of the diagram. In fact, an hcp phase appears below 51 K,[24] and other pseudopotential models correctly predict hcp stability.[25] There is no experimental evidence of a high-pressure transition at room temperature. Since sodium is a very good example of a nearly-free-electron metal, pseudopotential theory is expected to work well. It is therefore of interest to compare theoretical melting curves for different liquid models. Three theoretical melting curves are shown, based on the OCP, soft-sphere,[20] and hard-sphere[20] variational fluid models. It is clear that the OCP fluid model is in best agreement with experiment and has the lowest free energy of the three models.

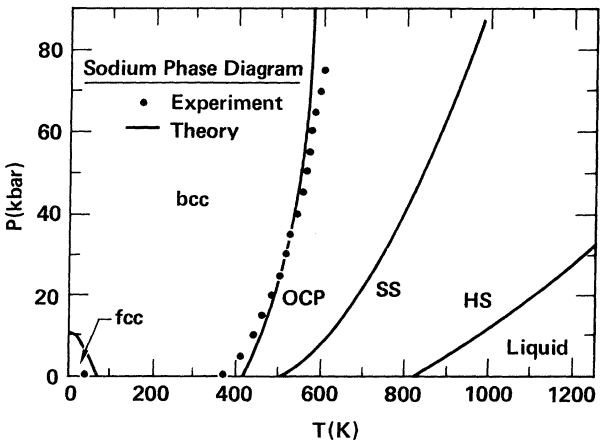

FIG. 6. Comparison of experimental and theoretical phase diagrams for sodium. Sodium shows a bcc to hcp transition near 40 K and $p=0$. The theoretical melting curves based on three different liquid models are shown. OCP denotes one-component plasma, SS denotes soft sphere, and HS, hard sphere.

Melting-curve calculations employing methods similar to ours have been reported by Stroud and Ashcroft[26] for Na. They calculated the solid properties using a self-consistent Debye method and the liquid properties using the hard-sphere variational theory. Stroud and Ashcroft's theoretical melting curve is in good agreement with experiment at $p=0$, but increases too slowly in pressure with increasing temperature.

The phase diagram for potassium is shown in Fig. 7. No close-packed phase is predicted at low temperature, and none is in fact observed.[24] It is interesting that the theory predicts a maximum in the melting temperature of 520 K at $p=55$ kbar. Above this pressure the slope $(\partial p/\partial T)$ of the predicted curve is negative. This is a somewhat unexpected result which probably arises from the softness of the effective ion-ion potential. Although the experimental melting temperature[13] appears to be constant at the highest pressures, thus suggesting a melting maximum in agreement with the theory, these experimental data are not considered reliable.[27]

The volumetric properties along the melting curve are also of interest. In Fig. 8, the melting temperature T_m is plotted against the midline volume, $V_m=0.5(V_s+V_l)$ for both experiment[14,15] and theory. There are significant quantitative differences, but the same approximately linear dependence is seen in both experiment and theory.

It should be noted that the OCP variational parameter Γ' does not have the scaling property of the hard-sphere reference fluid, where the packing fraction $\eta=\pi\sigma^3N/6V$ is nearly constant ($\eta=0.45$) along the melting curve. The parameter Γ' will in fact increase with pressure and exceed the value of the OCP freezing transition[21] at $\Gamma\approx 178$.

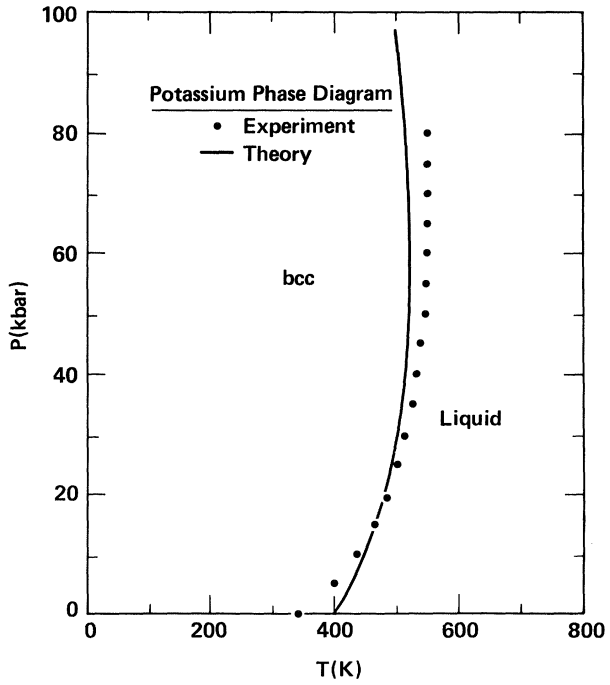

FIG. 7. Comparison of experimental and theoretical phase diagrams for potassium.

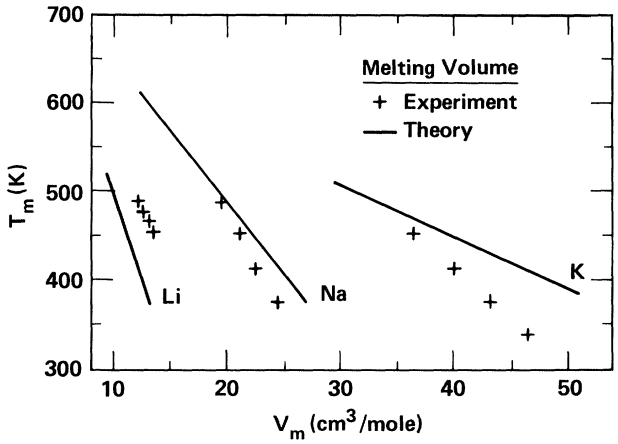

FIG. 8. Melting temperature vs the midline volume for Li, Na, and K. Experiment and theory are compared.

Overall, considering the very high precision in free energies required for accurate predictions, the theoretical phase boundaries are in good agreement with experiment. The agreement is especially remarkable for the solid-solid transitions considering the extremely small volume and energy changes across the transitions.

C. Very high compression

Experimental shock compression of alkali metals yields a more sensitive test of the pseudopotential theory for small interionic separations than static compression data because the high temperatures generated in the shock pro-

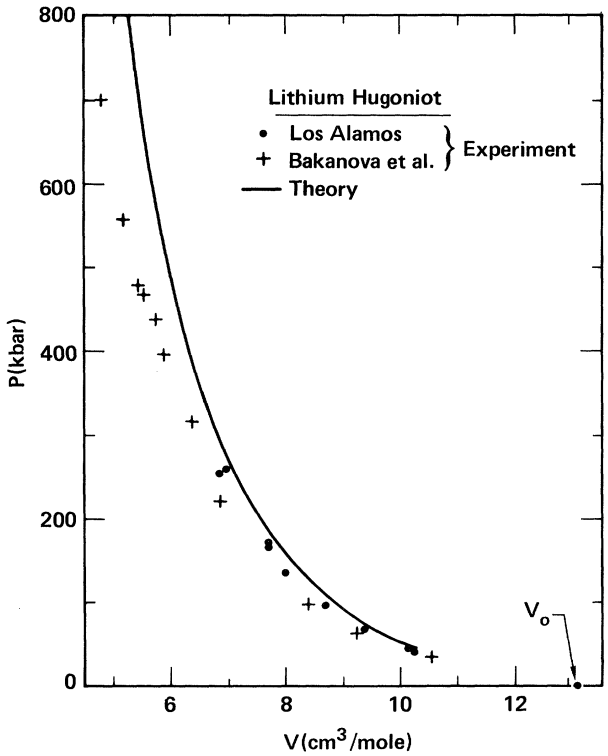

FIG. 9. Comparison of experimental and theoretical shock-compression Hugoniot curves for lithium.

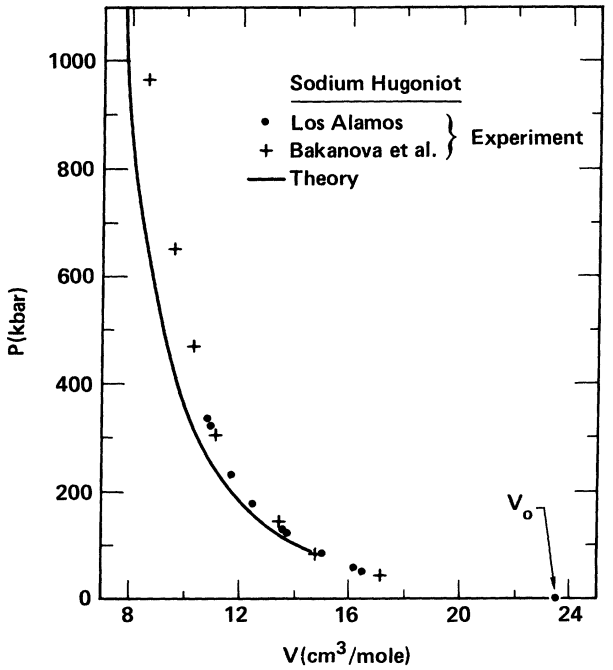

FIG. 10. Comparison of experimental and theoretical shock-compression Hugoniot curves for sodium.

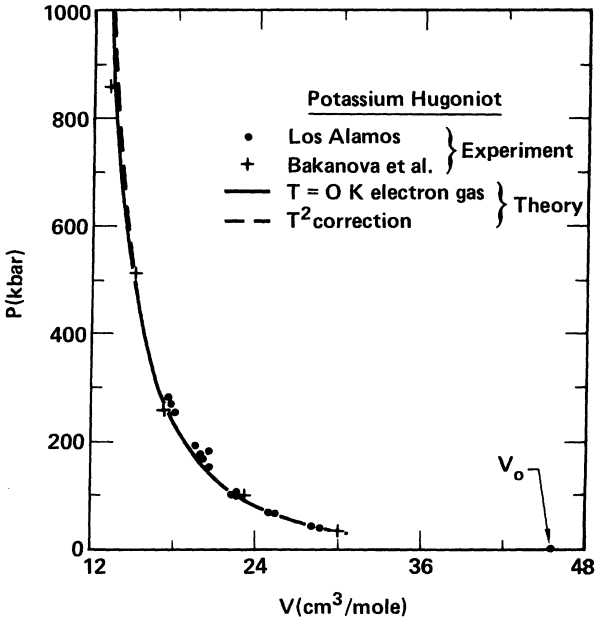

FIG. 11. Comparison of experimental and theoretical shock-compression Hugoniot curves for potassium. The theoretical results assuming a $T=0$ electron gas and assuming a T^2 correction are shown.

cess permit the ions to approach each other more closely.

The shock-compression curves (Hugoniot curves) of Li, Na, and K have been measured up to nearly 1 Mbar.[16,17] Because of shock heating,[7] these experimental points are largely in the liquid state, and they are compared with the predictions of the OCP fluid model. Hugoniot curves are calculated by solving the equation $E=E_0+0.5(p+p_0)\times(V_0-V)$, where the subscript indicates the initial conditions. Theory and experiment are compared in Figs. 9–11 and the theoretical calculations are summarized in Tables II–IV. The calculations include thermal excitation of the electron gas to order T^2, but this contribution makes a noticeable difference only in K, as shown in Fig. 11. In general the agreement is mixed. The theoretical Hugoniot curve is in good agreement with experiment for K, but it is too soft for Na and too stiff for Li. In the case of Li, our results are in better agreement with the Los Alamos shock data[16] than with the Soviet data.[17] The Soviet pressures are significantly lower, and even fall below the isothermal data of Olinger and Shaner.[9] This suggests that the Soviet shock data for Li are in error.

A very useful thermodynamic function is the lattice Grüneisen parameter, defined by

$$\gamma(V)=-\frac{1}{3N}\sum_{i=1}^{3N}\frac{\partial \ln \nu_i}{\partial \ln V}\,. \tag{19}$$

This function varies as the second derivative of pressure with volume[10] and is therefore a sensitive measure of the equation of state. Standard calculations[10,11] of $\gamma(V)$ indicate a smooth decrease with compression to a limit of 0.5. The lattice γ functions predicted from pseudopotential theory are shown in Fig. 12. They are in rough agreement with measured values at $V=V_0$, but they decrease to anomalously low values with compression.

Some insight into these results can be gained by com-

TABLE II. Isothermal and Hugoniot properties for lithium. Isothermal pressures (p), Grüneisen parameters (γ), Hugoniot temperatures (T_H) and pressures (p_H) are listed. For the Hugoniot-curve data, both the $T=0$ electron gas (unprimed) and the T^2 correction (primed) are included.

V/V_0	V (cm³/mol)	p (kbar)	γ	T_H (K)	p_H (kbar)	T_H' (K)	p_H' (kbar)
1.0	13.02	0.2	1.017				
0.9	11.72	15.8	0.955				
0.8	10.42	41.0	0.902				
0.7	9.11	83.4	0.854				
0.6	7.81	156.7	0.796	1006	176.6	996	176.6
0.5	6.51	293.5	0.722	2886	361.2	2802	361.2
0.4	5.21	576.8	0.647	11189	848.2	9859	848.6
0.3	3.91	1259.3	0.519	83590	3390.8	53210	3481.4

TABLE III. Isothermal and Hugoniot properties for sodium. Isothermal pressures (p), Grüneisen parameters (γ), Hugoniot temperatures (T_H), and pressures (p_H) are listed. For the Hugoniot-curve data, both the $T=0$ electron gas (unprimed) and the T^2 correction (primed) are included.

V/V_0	V (cm^3/mol)	p (kbar)	γ	T_H (K)	p_H (kbar)	T_H' (K)	p_H' (kbar)
1.0	23.79	−0.4	0.951				
0.9	21.41	7.7	0.907				
0.8	19.03	20.9	0.861				
0.7	16.65	43.1	0.797				
0.6	14.27	82.4	0.715	926	91.6	914	91.6
0.5	11.90	156.7	0.637	2644	186.7	2544	186.8
0.4	9.52	312.1	0.515	10219	432.1	8754	433.5
0.3	7.14	685.9	0.273	76972	1712.1	44931	1772.2

puting the effective ion-ion pair potential as follows:

$$\phi(r)=\frac{Z^2}{2r}+\frac{4Z^2}{\pi}\int_0^\infty f(q)\left[\frac{1}{\epsilon(q)}-1\right]\left[\frac{\sin(qr)}{qr}\right]dq \quad (20)$$

(in Ry), where r is the interionic separation. The pair potentials for the three metals are plotted semilogarithmically in Fig. 13. The pair potential has the expected repulsive form at small r, but it also displays a region of negative curvature most noticeable for K. The effect of this potential "softening" is first seen in the melting maximum predicted for K. If we take the effective interionic separation r_H along the Hugoniot curve to be given by $\phi(r_H)=(3/2)kT_H'$, then from Tables II–IV and Fig. 13, it is clear that the experimental shock data lie within the region of negative curvature. It is likely that the discrepancies between theoretical and experimental Hugoniot curves arise from this feature of the potential. The $\gamma(V)$ anomalies are also correlated with the negative curvature of the potential as well as with the tendency of the potential to decrease with compression through the volume dependence of $\epsilon(q)$ (shown for Li in Fig. 13). At sufficiently high compression in Na and K, this leads to $\gamma(V)<0$ and to imaginary lattice-vibration frequencies.

Since very similar $\gamma(V)$ functions are obtained by Vaks *et al.*,[5] who used different potentials and dielectric functions, it appears that this unrealistic behavior is independent of the details of the pseudopotential and the dielectric function.

It is clear from this discussion that the local pseudopotential theory is not adequate for ultrahigh pressure calculations, and that significant modifications in the theory are needed.

IV. DISCUSSION

In this paper we have used the experimental room-temperature isotherms of Li, Na, and K to determine the two-parameter Heine-Abarenkov local pseudopotential, and have then compared predictions with experiment in other regions of V,T space.

The predicted phase diagrams are in good agreement with experiment, which suggests that a pseudopotential fitted to experimental isotherms, together with accurate statistical-mechanical theories, will yield accurate phase boundaries. The p-T melting curves appear to be the most accurate so far computed from theory, although there is still room for improvement, as suggested by Fig. 8.

The effective pair potential which results from the screened pseudopotential shows unrealistic softening, leading to a $\gamma(V)$ which becomes negative at high compression. This anomalous behavior reflects the main weakness in the theory, and is probably also responsible for the substantial disagreements between theoretical and experimental Hugoniot-curve data.

This problem appears to be an artifact of the local pseudopotential model, in which valence charge density in the atomic core is not realistically calculated. Two ideas for eliminating this problem without changing the theoretical framework come to mind. The first is to add a repulsive term, such as a Born-Mayer exponential, to the pair potential. This approach is widely used in the literature[3] and

TABLE IV. Isothermal and Hugoniot properties for potassium. Isothermal pressures (p), Grüneisen parameters (γ), Hugoniot temperatures (T_H), and pressures (p_H) are listed. For the Hugoniot-curve data, both the $T=0$ electron gas (unprimed) and the T^2 correction (primed) are included.

V/V_0	V (cm^3/mol)	p (kbar)	γ	T_H (K)	p_H (kbar)	T_H' (K)	p_H' (kbar)
1.0	45.61	0.3	0.923				
0.9	41.05	4.4	0.870				
0.8	36.49	11.2	0.792				
0.7	31.93	22.8	0.704				
0.6	27.37	43.6	0.626	887	47.1	869	47.1
0.5	22.80	83.1	0.503	2458	93.9	2339	94.1
0.4	18.24	164.3	0.249	9329	210.2	7767	212.3
0.3	13.68	351.9	−0.518	71430	822.0	37239	857.7

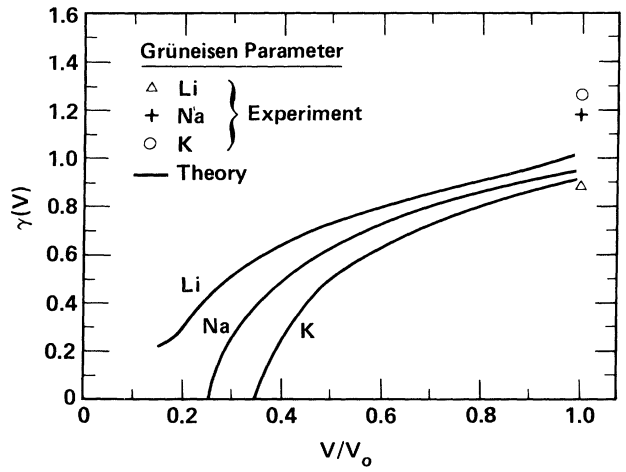

FIG. 12. Theoretical Grüneisen parameters vs relative volume for Li, Na, and K. Experimental values are shown at $V=V_0$.

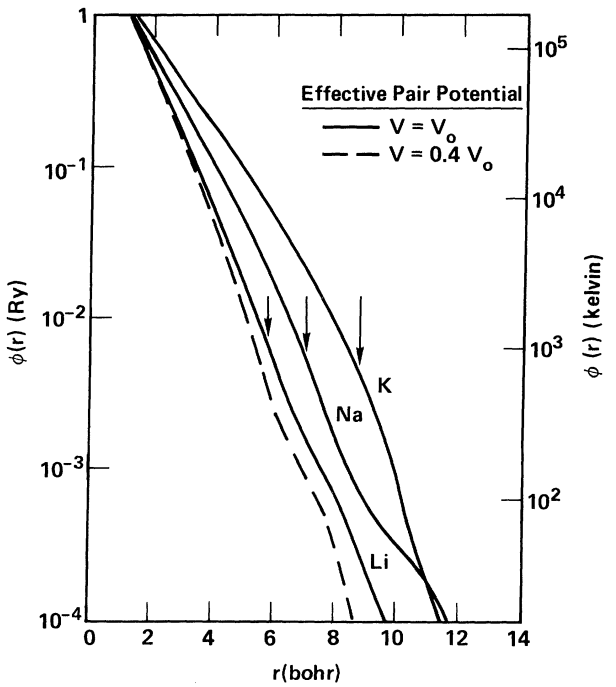

FIG. 13. Effective ion-ion pair potentials for lithium, sodium and potassium at their normal volumes, and at $V=0.4V_0$ for lithium. Nearest-neighbor distances at $V=V_0$ are marked with arrows.

is considered to represent repulsion due to core overlap. However, there is little physical justification for this claim, and such a term should be considered purely empirical. This approach has been used to obtain good theoretical agreement with experimental Hugoniot curves.[7] Another approach would be to make the coefficients in the pseudopotential volume dependent so that the potential becomes more positive (repulsive) with compression.

A more fundamental solution to the problem would be to relax the assumption of pseudopotential locality and adopt a nonlocal model. A recent calculation[28] of $\gamma(V)$ for K with such a model in fact shows no anomaly.

Improvements are also possible in the statistical-mechanical theories. Anharmonic effects in the solid are not negligible and should be included. The OCP variational theory needs further analysis as to its accuracy. For example, a still more accurate OCP $S_0(q,\Gamma')$ function might make noticeable differences in the liquid free energies and thus lead to further improvements in the theoretical melting curves.

ACKNOWLEDGMENTS

We thank F. J. Rogers for his calculations with the HNC model, B. Olinger for releasing his experimental data on Li and Na prior to publication, and R. Grover, J. Moriarty, H. DeWitt, and R. Boehler for valuable discussions. This work was performed under the auspices of the U.S. Department of Energy by Lawrence Livermore National Laboratory under Contract No. W-7405-Eng-48.

[1]M. Shimoji, *Liquid Metals* (Academic, London, 1977).
[2]N. W. Ashcroft and D. Stroud, Solid State Phys. 33, 1 (1978).
[3]D. C. Wallace, *Thermodynamics of Crystals* (Wiley, New York, 1972).
[4]M. Senoo, H. Mii, and I. Fujishiro, J. Phys. Soc. Jpn. 41, 1562 (1976).
[5]V. G. Vaks, S. P. Kravchuk, and A. V. Trefilov, Fiz. Tverd. Tela 19, 1271 (1977) [Sov. Phys.—Solid State 19, 740 (1977)].
[6]T. Soma, J. Phys. F 10, 1401 (1980).
[7]M. Ross, Phys. Rev. B 21, 3140 (1980).
[8]S. N. Vaidya, I. C. Getting, and G. C. Kennedy, J. Phys. Chem. Solids 32, 2545 (1971).
[9]B. Olinger and J. W. Shaner, (Li) Science 219, 1071 (1983); B. Olinger, (Na) (unpublished).
[10]R. Grover, R. N. Keeler, F. J. Rogers, and G. C. Kennedy, J. Phys. Chem. Solids 30, 2091 (1969).
[11]R. Grover (personal communication) has developed a model which combines the compressibility theory of the Grüneisen parameter with the experimentally measured value at $V=V_0$. This technique is used to reduce shock-compression Hugoniot-curve data to room-temperature isotherms. These results are shown in Figs. 1–3.
[12]I. N. Makarenko, A. M. Nikolaenko, and S. M. Stishov, in *Liquid Metals, 1976,* edited by R. Evans and D. Greenwood, (Institute of Physics, Bristol, 1977), p. 79.
[13]H. D. Luedemann and G. C. Kennedy, J. Geophys. Res. 73, 2795 (1968).
[14]S. M. Stishov, Usp. Fiz. Nauk 114, 3 (1974) [Sov. Phys.—Usp. 17, 625 (1975)].
[15]I. N. Makarenko, A. M. Nikolaenko, and S. M. Stishov, Zh. Eksp. Teor. Fiz. 74, 2175 (1978) [Sov. Phys.—JETP 47, 1132 (1978)].
[16]*LASL Shock Hugoniot Data,* edited by S. P. Marsh (University of California Press, Berkeley, 1980).
[17]A. A. Bakanova, I. P. Dudoladov, and R. F. Trunin, Fiz. Tverd. Tela 7, 1615 (1965) [Sov. Phys.—Solid State 7, 1307 (1965)].
[18]S. Rahman and G. Vignale, J. Phys. F 12, L41 (1982).

[19]L. L. Foldy, Phys. Rev. B 17, 4889 (1978).
[20]M. Ross, H. E. DeWitt, and W. B. Hubbard, Phys. Rev. A 24, 1016 (1981).
[21]W. L. Slattery, G. D. Doolen, and H. E. DeWitt, Phys. Rev. A 26, 2255 (1982). There are slight differences between the values of the coefficients we used and those in the final version of Slattery *et al.*'s paper.
[22]Y. Rosenfeld and N. W. Ashcroft, Phys. Rev. A 20, 1208 (1979).
[23]W. A. Harrison, *Electronic Structure and the Properties of Solids* (Freeman, San Francisco, 1980), Chaps. 15—17.
[24]J. Donohue, *The Structures of the Elements* (Wiley, New York, 1974).
[25]J. A. Moriarty, Phys. Rev. B 26, 1754 (1982).
[26]D. Stroud and N. W. Ashcroft, Phys. Rev. B 5, 371 (1972).
[27]R. Boehler, private communication.
[28]J. Moriarty, private communication.